Available online at www.sciencedirect.com
SCIENCE DIRECT®
Journal of Solid State Chemistry 178 (2005) 2724–2733
JOURNAL OF SOLID STATE CHEMISTRY
www.elsevier.com/locate/jssc

New rare earth metal-rich indides $RE_{14}Ni_3In_3$ (RE = Sc, Y, Gd–Tm, Lu)—synthesis and crystal chemistry

Mar'yana Lukachuk[a], Yaroslav V. Galadzhun[b], Roman I. Zaremba[c], Mariya V. Dzevenko[b], Yaroslav M. Kalychak[b], Vasyl I. Zaremba[b], Ute Ch. Rodewald[c], Rainer Pöttgen[c,*]

[a]*Max-Planck-Institut für Festkörperforschung, Heisenbergstrasse 1, D-70569 Stuttgart, Germany*
[b]*Inorganic Chemistry Department, Ivan Franko National University of Lviv, Kyryla and Mephodiya Street 6, 79005 Lviv, Ukraine*
[c]*Institut für Anorganische und Analytische Chemie and NRW Graduate School of Chemistry, Universität Münster, Corrensstrasse 30, D-48149 Münster, Germany*

Received 11 May 2005; received in revised form 13 June 2005; accepted 15 June 2005
Available online 21 July 2005

Abstract

The rare earth–nickel–indides $RE_{14}Ni_3In_3$ (RE = Sc, Y, Gd–Tm, Lu) were synthesized from the elements by arc-melting and subsequent annealing. The compounds were investigated on the basis of X-ray powder and single crystal data: $Lu_{14}Co_2In_3$ type, $P4_2/nmc$, $Z = 4$, $a = 888.1(1)$, $c = 2134.7(4)$, w$R2 = 0.0653$, 1381 F^2 values, 63 variables for $Sc_{13.89}Ni_{3.66}In_{2.45}$; $a = 961.2(1)$, $c = 2316.2(5)$, w$R2 = 0.0633$, 1741 F^2 values, 64 variables for $Y_{13.84}Ni_{3.19}In_{2.97}$; $a = 965.3(1)$, $c = 2330.5(5)$, w$R2 = 0.0620$, 1765 F^2 values, 63 variables for $Gd_{14}Ni_{3.29}In_{2.71}$; $a = 956.8(1)$, $c = 2298.4(5)$, w$R2 = 0.0829$, 1707 F^2 values, 64 variables for $Tb_{13.82}Ni_{3.36}In_{2.82}$; $a = 951.7(1)$, $c = 2289.0(5)$, w$R2 = 0.0838$, 1794 F^2 values, 64 variables for $Dy_{13.60}Ni_{3.34}In_{3.06}$; $a = 948.53(7)$, $c = 2270.6(1)$, w$R2 = 0.1137$, 1191 F^2 values, 64 variables for $Ho_{13.35}Ni_{3.17}In_{3.48}$; $a = 943.5(1)$, $c = 2269.1(5)$, w$R2 = 0.0552$, 1646 F^2 values, 64 variables for $Er_{13.53}Ni_{3.14}In_{3.33}$; $a = 938.42(7)$, $c = 2250.8(1)$, w$R2 = 0.1051$, 1611 F^2 values, 64 variables for $Tm_{13.47}Ni_{3.28}In_{3.25}$; $a = 937.3(1)$, $c = 2249.6(5)$, w$R2 = 0.0692$, 1604 F^2 values, 64 variables for $Tm_{13.80}Ni_{3.49}In_{2.71}$; and $a = 933.4(1)$, $c = 2263.0(5)$, w$R2 = 0.0709$, 1603 F^2 values, 64 variables for $Lu_{13.94}Ni_{3.07}In_{2.99}$. The $RE_{14}Ni_3In_3$ indides show significant Ni/In mixing on the 4c In1 site. Except the gadolinium compound, the $RE_{14}Ni_3In_3$ intermetallics also reveal RE/In mixing on the 4c RE1 site, leading to the refined compositions. Due to the high rare earth metal content, the seven crystallographically independent RE sites have between 9 and 10 nearest RE neighbors. The $RE_{14}Ni_3In_3$ structures can be described as a complex intergrowth of rare earth-based polyhedra. Both nickel sites have a distorted trigonal-prismatic rare earth coordination. An interesting feature is the In2–In2 dumb-bell at an In2–In2 distance of 304 pm (for $Gd_{14}Ni_{3.29}In_{2.71}$). The crystal chemical peculiarities of the $RE_{14}Ni_3In_3$ indides are briefly discussed.

Keywords: Intermetallic compounds; Crystal structure; Indium

1. Introduction

Ternary rare earth (RE)–transition metal (T)–indides $RE_xT_yIn_z$ display a peculiar crystal chemistry [1]. If x, y, and z have almost similar values, the transition metal and indium atoms build up two- or three-dimensional $[T_yIn_z]$ polyanionic networks in which the rare earth atoms fill cages or channels. If the indium content of such intermetallics is significantly increased, the structural building principle remains almost the same, however, the indium atoms build up indium substructures within the three-dimensional $[T_yIn_z]$ polyanions

*Corresponding author. Fax: +49 251 83 36002.
E-mail addresses: kalychak@franko.lviv.ua (Y.M. Kalychak), pottgen@uni-muenster.de (R. Pöttgen).

0022-4596/$ - see front matter © 2005 Elsevier Inc. All rights reserved.
doi:10.1016/j.jssc.2005.06.021

which resemble the elemental indium structure, i.e. distorted indium cubes. An overview of these substructures is given in [1–3].

The situation is different, if the transition metal or the rare earth metal contents are very high. In the case of *T*-rich indides, the transition metal atoms show different kinds of one-, two-, or three-dimensional *T*-clusters. Interesting examples are the structures of $LaNi_2In$, $CeNi_4In$, $Ce_4Ni_7In_8$, and $LaNi_7In_6$ [4]. With a high rare earth metal content, there exist only few structural series of such compounds: $RE_{12}Ni_6In$ (RE = Y, La, Pr, Nd, Sm, Gd) and $RE_{12}Co_6In$ (RE = La, Pr, Nd, Sm) with $Sm_{12}Ni_6In$ type [5–7], RE_6Co_2In (RE = Y, Sm, Gd–Ho, Tm, Lu) with Ho_6Co_2Ga structure [7,8], $RE_{14}Co_2In_3$ (RE = Y, Gd–Tm, Lu) [9] with $Lu_{14}Co_2In_3$ type, Er_5Ni_2In and $Tm_{4.83(3)}Ni_2In_{1.17(3)}$ [10] with Mo_5SiB_2 structure, and the series $RE_{12}Pt_7In$ (RE = Ce, Pr, Nd, Gd, Ho) [11] with an ordered version of the Gd_3Ga_2 type. All these intermetallics have high coordination numbers and chemical bonding is significantly governed by the many *RE*–*RE* contacts. The structures can be described by a complex packing pattern of different polyhedra [6,7].

Recently Canepa et al. [12] reported a single crystal study of the gadolinium-based indide $Gd_{14}Co_3In_{2.7}$. The latter compound is related to the $Lu_{14}Co_2In_3$ type indides, however, the gadolinium compound shows an additional 4*d* Co2 site, defects on the 8*g* Co1 site, and a mixed Co/In occupancy on the 4*c* site. During our systematic phase analytical studies of the *RE*–Ni–In systems [4,13–19], we found a family of new nickel compounds $RE_{14}Ni_3In_3$ (RE = Sc, Y, Gd–Tm, Lu), which form only with the smaller rare earth elements. These indides also show an additional 4*d* Ni2 site, similar to $Gd_{14}Co_3In_{2.7}$ [12], but also some *RE*/In mixing of the 4*c* *RE*1 sites. The synthesis, crystal growth, structure determination and crystal chemistry of these phases are reported herein. A preliminary account of some of this work was given recently at a conference [20].

Besides the structural chemistry described herein, the main interest in such materials concerns their magnetic and electrical properties. Especially the gadolinium-based materials are promising candidates for magnetic refrigeration devices, e.g. the isotypic cobalt compound $Gd_{14}Co_3In_{2.7}$ [12] was investigated along that line.

2. Experimental

2.1. Synthesis

Starting materials for the preparation of the $RE_{14}Ni_3In_3$ intermetallics with RE = Sc, Y, Gd–Tm, Lu) were ingots of the rare earth elements (Chempur, Johnson Matthey, or Kelpin), nickel wire (∅ 0.38 mm, Johnson-Matthey) or nickel powder (Johnson-Matthey), and indium tear drops (Johnson-Matthey), all with stated purities better than 99.9%. All samples were prepared directly from the elements via arc-melting [21] under an atmosphere of ca. 600 mbar argon. The argon was purified before over titanium sponge (900 K), silica gel, and molecular sieves. Except the thulium-based compounds, the elements were weighed in the ideal 14:3:3 atomic ratios. Two samples with thulium were prepared with the starting compositions Tm:Ni:In of 66:29:5 and 67:22:11. All samples were turned over and remelted two times in the arc-melting crucible in order to achieve homogeneity. The weight losses were always smaller than 0.5 wt%.

The $RE_{14}Ni_3In_3$ indides were obtained only in polycrystalline form after the arc-melting procedures. These samples were then sealed in tantalum tubes under an argon pressure of ca. 800 mbar. The tantalum ampoules were subsequently enclosed in evacuated silica ampoules for oxidation protection and the samples were heated in a box furnace at 1270 K for 3 h, then cooled at a rate of 5 K/h to 870 K and held at that temperature for 24 h. Finally the samples were cooled to room temperature within 3 h. This procedure led to the formation of crystals, suitable for intensity data collections. The silvery brittle samples were stable in moist air over months. Powders of the $RE_{14}Ni_3In_3$ indides are dark gray. Single crystals exhibit metallic luster.

2.2. X-ray powder diffraction and scanning electron microscopy

All samples were investigated by Guinier powder diffraction (imaging plate technique, Fujifilm BAS-1800) with Cu $K\alpha_1$ radiation and α-quartz (a = 491.30, c = 540.46 pm) as an internal standard. The tetragonal lattice parameters (Table 1) were obtained from least-squares fits of the Guinier data. The indexing of the complex powder patterns was facilitated through intensity calculations [22] using the positional parameters of the structure refinements.

The crystals investigated on the diffractometers have been analyzed in a scanning electron microscope (LEICA 420i) through energy dispersive analyses of X-rays. The rare earth trifluorides, nickel metal, and InAs were used as standards. No impurity elements heavier than sodium have been observed. The experimentally determined compositions were close to the compositions calculated from the structure refinements. To give an example, the scandium-containing crystal had a refined composition of 69.5 at% Sc:18.3 at% Ni:12.2 at% In, as compared to the EDX data of 70 ± 1 at% Sc:17 ± 1 at% Ni:13 ± 1 at% In. The standard uncertainty accounts for the various point measurements.

Table 1
Lattice parameters of the tetragonal metal-rich indides $RE_{14-x}Ni_{3+y}In_{3+x-y}$ (RE = Sc, Y, Gd–Tm, Lu)

Starting composition	Refined composition	a (pm)	c (pm)	V (nm^3)
14Sc: 3Ni:3In[a]		888.13(6)	2134.1(2)	1.6834
	$Sc_{13.89(1)}Ni_{3.66(1)}In_{2.45(1)}$[b]	888.1(1)	2134.7(4)	1.6838
14Y:3Ni:3In[a]		961.07(8)	2315.5(2)	2.1387
	$Y_{13.84(2)}Ni_{3.19(2)}In_{2.97(2)}$[b]	961.2(1)	2316.2(5)	2.1398
14Gd:3Ni:3In[a]		965.3(2)	2332.7(6)	2.1737
	$Gd_{14}Ni_{3.29(2)}In_{2.71(2)}$[b]	965.3(1)	2330.5(5)	2.1716
14Tb:3Ni:3In[a]		956.59(8)	2296.7(4)	2.1016
	$Tb_{13.82(2)}Ni_{3.36(2)}In_{2.82(2)}$[b]	956.8(1)	2298.4(5)	2.1042
14Dy:3Ni:3In[a]		952.1(1)	2290.0(5)	2.0759
	$Dy_{13.60(2)}Ni_{3.34(2)}In_{3.06(2)}$[b]	951.7(1)	2289.0(5)	2.0730
14Ho:3Ni:3In[a]		949.95(7)	2291.7(3)	2.0680
	$Ho_{13.35(2)}Ni_{3.17(2)}In_{3.48(2)}$[b]	948.53(7)	2270.6(1)	2.0429
14Er:3Ni:3In[a]		944.23(9)	2259.9(5)	2.0149
	$Er_{13.53(2)}Ni_{3.14(2)}In_{3.33(2)}$[b]	943.5(1)	2269.1(5)	2.0201
66Tm:29Ni:5In[a]		939.18(5)	2251.2(2)	1.9857
	$Tm_{13.47(3)}Ni_{3.28(3)}In_{3.25(3)}$[b]	938.42(7)	2250.8(1)	1.9822
67Tm:22Ni:11In[a]		937.48(9)	2247.9(4)	1.9756
	$Tm_{13.80(2)}Ni_{3.49(2)}In_{2.71(2)}$[b]	937.3(1)	2249.6(5)	1.9761
14Lu:3Ni:3In[a]		934.18(9)	2265.9(4)	1.9774
	$Lu_{13.94(2)}Ni_{3.07(2)}In_{2.99(4)}$[b]	933.4(1)	2263.0(5)	1.9716

[a]Lattice parameters from Guinier powder data.
[b]Lattice parameters from diffractometer measurements.

2.3. Structure refinements

Small irregularly shaped single crystals were selected from the annealed crushed samples and first examined on Buerger precession cameras (white Mo radiation, Fujifilm BAS-1800 imaging plate system) in order to check the quality for intensity data collection. From oriented Laue photographs, tetragonal symmetry (4-fold axis) was evident. The image plates for the Buerger photographs were exposed up to 10 min. No diffuse scattering was evident.

Single crystal intensity data of $Ho_{13.35}Ni_{3.17}In_{3.48}$ and $Tm_{13.47}Ni_{3.28}In_{3.25}$ were collected at room temperature by use of a four-circle diffractometer (CAD4) with graphite monochromatized Mo-$K\alpha$ (71.073 pm) radiation and a scintillation counter with pulse height discrimination. Scans were taken in the $\omega/2\theta$ mode. Empirical absorption corrections were applied on the basis of Ψ-scan data followed by a spherical absorption correction, as implemented in the diffractometer software. The intensity data of the other indides were collected at room temperature by use of a Stoe IPDS-II image plate diffractometer in oscillation mode. The absorption corrections were numerical. All relevant crystallographic data for the data collections and evaluations are listed in Tables 2–4.

The close structural relationship with $Lu_{14}Co_2In_3$ [9] and $Gd_{14}Co_3In_{2.7}$ [12] was already evident from the Guinier powder data. Analyses of the diffractometer data sets were compatible with space group $P4_2/nmc$, in agreement with the previous investigations. The atomic parameters of $Lu_{14}Co_2In_3$ [9] were taken as starting values and the structures were refined with SHELXL-97 (full-matrix least-squares on F^2) [23] with anisotropic displacement parameters for all atoms. For all data sets, the difference Fourier synthesis clearly revealed the additional 4d Ni2 site.

In separate series of least-squares cycles we have then refined the occupancy parameters in order to check for the correct composition and the correct site assignment. Similar to $Gd_{14}Co_3In_{2.7}$ [12], the 4c In1/Ni3 sites also show mixed indium/nickel occupancy. While the gadolinium-based crystal showed full occupancy within two standard deviations for all other sites, the 4c RE1 sites of the remaining crystals revealed mixed RE/In occupancies. In the final cycles, these occupancies were refined as a least-squares variable, leading to the compositions listed in Table 5 for the crystals investigated. Two thulium-based crystals from two samples with slightly different starting compositions (see Section 2.1) were investigated. These crystals showed different occupancies for both the 4c Tm and the 4c In sites, leading to a different Tm/In and In/Ni mixing and thus to different compositions. The final difference Fourier syntheses were flat for all data sets (Tables 2–4). The positional parameters of the refinements are listed in Table 5. Exemplary, the interatomic distances of $Gd_{14}Ni_{3.29}In_{2.71}$ are listed in

Table 2
Crystal data and structure refinements for $Sc_{13.89(1)}Ni_{3.66(1)}In_{2.45(1)}$, $Y_{13.84(2)}Ni_{3.19(2)}In_{2.97(2)}$, and $Gd_{14}Ni_{3.29(2)}In_{2.71(2)}$, space group $P4_2/nmc$, $Z = 4$

Empirical formula	$Sc_{13.89(1)}Ni_{3.66(1)}In_{2.45(1)}$	$Y_{13.84(2)}Ni_{3.19(2)}In_{2.97(2)}$	$Gd_{14}Ni_{3.29(2)}In_{2.71(2)}$
Molar mass (g/mol)	1120.76	1758.81	2705.54
Unit cell dimensions	See Table 1	See Table 1	See Table 1
Calculated density (g/cm^3)	4.42	5.46	8.28
Crystal size (μm^3)	$60 \times 40 \times 20$	$70 \times 50 \times 40$	$80 \times 80 \times 30$
Detector distance (mm)	60	80	80
Exposure time (min)	42	32	12
ω range; increment (deg)	0–180; 1.0	0–180; 1.0	0–180; 1.0
Integr. param. A, B, EMS	14.8; 1.1; 0.009	10.2; 2.1; 0.016	11.0; 2.0; 0.010
Transm. ratio (max/min)	1.53	1.59	2.86
Absorption coefficient (mm^{-1})	12.4	42.8	47.6
$F(000)$	2057	3098	4483
θ range (deg)	3–30	2–30	2–30
Range in $h\,k\,l$	± 12, ± 12, $-30 \leqslant l \leqslant 27$	± 13, ± 13, ± 32	± 13, ± 13, ± 32
Total no. reflections	14 041	21 364	21 831
Independent reflections	1381 ($R_{int} = 0.0964$)	1741 ($R_{int} = 0.1494$)	1765 ($R_{int} = 0.1091$)
Reflections with $I > 2\sigma(I)$	1163 ($R_{sigma} = 0.0380$)	1312 ($R_{sigma} = 0.0584$)	1612 ($R_{sigma} = 0.0506$)
Data/parameters	1381/63	1741/64	1765/63
Goodness-of-fit on F^2	1.331	1.068	1.211
Final R indices [$I > 2\sigma(I)$]	$R_1 = 0.0571$ $wR_2 = 0.0631$	$R_1 = 0.0413$ $wR_2 = 0.0586$	$R_1 = 0.0286$ $wR_2 = 0.0601$
R indices (all data)	$R_1 = 0.0735$ $wR_2 = 0.0653$	$R_1 = 0.0666$ $wR_2 = 0.0633$	$R_1 = 0.0337$ $wR_2 = 0.0620$
Extinction coefficient	—	0.00016(2)	0.00049(2)
Largest diff. peak and hole (e/Å^3)	2.13/ −1.25	2.17/ −1.27	3.88/ −2.89

Table 3
Crystal data and structure refinements for $Tb_{13.82(2)}Ni_{3.36(2)}In_{2.82(2)}$, $Dy_{13.60(2)}Ni_{3.34(2)}In_{3.06(2)}$, and $Ho_{13.35(2)}Ni_{3.17(2)}In_{3.48(2)}$, space group $P4_2/nmc$, $Z = 4$

Empirical formula	$Tb_{13.82(2)}Ni_{3.36(2)}In_{2.82(2)}$	$Dy_{13.60(2)}Ni_{3.34(2)}In_{3.06(2)}$	$Ho_{13.35(2)}Ni_{3.17(2)}In_{3.48(2)}$
Molar mass (g/mol)	2718.26	2773.03	2787.89
Unit cell dimensions	See Table 1	See Table 1	See Table 1
Calculated density (g/cm^3)	8.58	8.89	9.06
Crystal size (μm^3)	$80 \times 50 \times 20$	$95 \times 70 \times 35$	$20 \times 20 \times 30$
Detector distance (mm)	75	90	—
Exposure time (min)	28	20	—
ω range; increment (deg)	0–180; 1.0	0–180; 1.0	—
Integr. param. A, B, EMS	12.5; 2.0; 0.014	12.5; 2.5; 0.016	—
Transm. ratio (max/min)	2.08	3.09	1.93
Absorption coefficient (mm^{-1})	51.7	54.6	57.2
$F(000)$	4524	4588	4616
θ range (deg)	2–30	2–31	2–30
Range in $h\,k\,l$	± 13, ± 13, ± 32	± 13, ± 13, $-32 \leqslant l \leqslant 27$	$0 \leqslant h \leqslant 4$, ± 13, ± 31
Total no. reflections	20 754	21 642	5091
Independent reflections	1707 ($R_{int} = 0.1248$)	1794 ($R_{int} = 0.1067$)	1191 ($R_{int} = 0.1312$)
Reflections with $I > 2\sigma(I)$	1571 ($R_{sigma} = 0.0469$)	1667 ($R_{sigma} = 0.0364$)	658 ($R_{sigma} = 0.0806$)
Data/parameters	1707/64	1794/64	1191/64
Goodness-of-fit on F^2	1.325	1.214	1.050
Final R indices [$I > 2\sigma(I)$]	$R_1 = 0.0345$ $wR_2 = 0.0812$	$R_1 = 0.0355$ $wR_2 = 0.0821$	$R_1 = 0.0451$ $wR_2 = 0.0839$
R indices (all data)	$R_1 = 0.0395$ $wR_2 = 0.0829$	$R_1 = 0.0397$ $wR_2 = 0.0838$	$R_1 = 0.1261$ $wR_2 = 0.1137$
Extinction coefficient	0.00023(2)	0.00024(2)	0.00010(2)
Largest diff. peak and hole (e/Å^3)	2.63/–2.54	4.64/–3.21	2.82/–3.33

Table 4
Crystal data and structure refinements for $Er_{13.53(2)}Ni_{3.14(2)}In_{3.33(2)}$, $Tm_{13.47(3)}Ni_{3.28(3)}In_{3.25(3)}$, $Tm_{13.80(2)}Ni_{3.49(2)}In_{2.71(2)}$, and $Lu_{13.94(2)}Ni_{3.07(2)}In_{2.99(2)}$, space group $P4_2/nmc$, $Z = 4$

Empirical formula	$Er_{13.53(2)}Ni_{3.14(2)}In_{3.33(2)}$	$Tm_{13.47(3)}Ni_{3.28(3)}In_{3.25(3)}$	$Tm_{13.80(2)}Ni_{3.49(2)}In_{2.71(2)}$	$Lu_{13.94(2)}Ni_{3.07(2)}In_{2.99(2)}$
Molar mass (g/mol)	2829.87	2841.09	2847.99	2963.33
Unit cell dimensions	See Table 1	See Table 1	See Table 1	See Table 1
Calculated density (g/cm^3)	9.31	9.52	9.57	9.98
Crystal size (μm^3)	$40 \times 30 \times 10$	$120 \times 80 \times 40$	$80 \times 50 \times 30$	$30 \times 60 \times 70$
Detector distance (mm)	60	—	60	70
Exposure time (min)	23	—	12	20
ω range; increment (deg)	0–180; 1.0	—	0–180; 1.0	0–180; 1.0
Integr. param. *A*, *B*, EMS	9.2; 0.1; 0.024	—	10.5; 2.5; 0.008	12.0; 3.0; 0.014
Transm. ratio (max/min)	2.34	2.32	2.67	1.94
Absorption coefficient (mm^{-1})	62.0	66.2	67.5	75.3
F(000)	4685	4722	4732	4890
θ range (deg)	3–30	2–30	2–30	2–30
Range in *h k l*	± 13, ± 13, $-31 \leqslant l \leqslant 28$	$+13$, $+13$, $+30$	± 13, ± 13, $-29 \leqslant l \leqslant 31$	± 13, ± 13, $-30 \leqslant l \leqslant 31$
Total no. reflections	19 241	3092	19 482	19 200
Independent reflections	1646 ($R_{int} = 0.1077$)	1611 ($R_{int} = 0.0726$)	1604 ($R_{int} = 0.1158$)	1603 ($R_{int} = 0.1144$)
Reflections with $I > 2\sigma(I)$	1415 ($R_{sigma} = 0.0398$)	1107 ($R_{sigma} = 0.0739$)	1462 ($R_{sigma} = 0.0424$)	1420 ($R_{sigma} = 0.0394$)
Data/parameters	1646/64	1611/64	1604/64	1603/64
Goodness-of-fit on F^2	1.126	1.027	1.190	0.916
Final *R* indices [$I > 2\sigma(I)$]	$R_1 = 0.0308$	$R_1 = 0.0413$	$R_1 = 0.0334$	$R_1 = 0.0304$
	$wR_2 = 0.0530$	$wR_2 = 0.0918$	$wR_2 = 0.0674$	$wR_2 = 0.0672$
R indices (all data)	$R_1 = 0.0410$	$R_1 = 0.0751$	$R_1 = 0.0389$	$R_1 = 0.0388$
	$wR_2 = 0.0552$	$wR_2 = 0.1051$	$wR_2 = 0.0692$	$wR_2 = 0.0709$
Extinction coefficient	0.00018(1)	0.00003(2)	0.00021(1)	0.00012(1)
Largest diff. peak and hole (e/Å^3)	2.96/ −2.27	5.08/ −4.69	5.10/ −2.81	2.16/ −2.19

Table 6. Further details on the structure refinements are available.[1]

3. Results and discussion

Eight rare earth metal-rich indides $RE_{14}Ni_3In_3$ have been synthesized and structurally characterized. These intermetallics are related to the recently reported series of cobalt compounds $RE_{14}Co_2In_3$ (RE = Y, Gd–Tm, Lu) [9]. A recent single crystal study on $Gd_{14}Co_3In_{2.7}$ [12] revealed an additional cobalt site 4*d*, defects on the 8*g* Co1 site, and a mixed In/Co occupancy for the 4*c* site. So far, only brief descriptions of the complex crystal structure of these compounds have been given [1,7,9,12].

In Fig. 1 we present a plot of the cell volumes of the series of $RE_{14}Ni_3In_3$ indides. The cell volume decreases from the gadolinium to the lutetium compound as expected from the lanthanoid contraction. The small discrepancies between the volumes determined from the powders and the single crystals reflect the homogeneity ranges. The volume of the yttrium compound fits in between the volumes of the gadolinium and terbium compounds as frequently observed for other series of metal-rich indides [1]. The scandium compound has the by far smallest cell volume in the series of $RE_{14}Ni_3In_3$ indides. Due to the high scandium content, the decrease of the cell volume from the lutetium to the scandium compound is remarkable.

The $RE_{14}Ni_3In_3$ indides show In1/Ni3 mixing for the gadolinium compound and additionally *RE*1/In3 mixing for all remaining compounds. We can thus write the general formula $RE_{14-x}Ni_{3+y}In_{3+x-y}$. For reasons of simplicity, in the following discussion we write only $RE_{14}Ni_3In_3$ and for a comparison of the interatomic distances we refer to the gadolinium compound which shows only In1/Ni3 mixing. From all crystals investigated, the one of $Lu_{13.94}Ni_{3.07}In_{2.99}$ shows the closest composition to the ideal one (14:3:3).

The complex structure of $Gd_{14}Ni_{3.29}In_{2.71}$ contains seven crystallographically independent gadolinium sites, two nickel sites, one mixed occupied site In1/Ni3 and one indium site (Table 5). The coordination polyhedra of the $Gd_{14}Ni_{3.29}In_{2.71}$ structure are presented in Fig. 2. The gadolinium atoms have between 12 and 15 nearest neighbors. Due to the high gadolinium content, between 9 and 10 of these neighbors are gadolinium atoms at Gd–Gd distances ranging from 347 to 392 pm, close to

[1]Details may be obtained from: Fachinformationszentrum Karlsruhe, D-76344 Eggenstein-Leopoldshafen (Germany), by quoting the Registry Nos. CSD–415387 ($Sc_{13.89}Ni_{3.66}In_{2.45}$), CSD–415388 ($Y_{13.84}Ni_{3.19}In_{2.97}$), CSD–415389 ($Gd_{14}Ni_{3.29}In_{2.71}$), CSD–415390 ($Tb_{13.82}Ni_{3.36}In_{2.82}$), CSD–415391 ($Dy_{13.60}Ni_{3.34}In_{3.06}$), CSD–415392 ($Ho_{13.35}Ni_{3.17}In_{3.48}$), CSD–415393 ($Er_{13.53}Ni_{3.14}In_{3.33}$), CSD–415394 ($Tm_{13.47}Ni_{3.28}In_{3.25}$), CSD–415395 ($Tm_{13.80}Ni_{3.49}In_{2.71}$), and CSD–415396 ($Lu_{13.94}Ni_{3.07}In_{2.99}$).

Table 5
Atomic coordinates and isotropic displacement parameters (pm^2) for $RE_{14-x}Ni_{3+y}In_{3+x-y}$ (RE = Sc, Y, Gd–Tm, Lu), space group $P4_2/nmc$. U_{eq} is defined as one third of the trace of the orthogonalized U_{ij} tensor

Atom	Wyckoff site	Occupancy/%	x	y	z	U_{eq}
$Sc_{13.89(1)}Ni_{3.66(1)}In_{2.45(1)}$						
Sc1/In3	4*c*	89.4(9)/10.6(9)	3/4	1/4	0.14492(10)	108(7)
Sc2	4*d*	100	1/4	1/4	0.21302(12)	90(4)
Sc3	8*g*	100	1/4	0.5482(2)	0.31101(10)	154(4)
Sc4	8*g*	100	1/4	0.56534(19)	0.98860(8)	107(3)
Sc5	8*f*	100	0.56141(12)	$-x$	1/4	92(3)
Sc6	8*g*	100	1/4	0.44434(18)	0.46704(8)	91(3)
Sc7	16*h*	100	0.43813(13)	0.43580(13)	0.10443(5)	86(2)
Ni1	8*g*	100	1/4	0.53460(13)	0.19192(6)	124(2)
Ni2	4*d*	100	1/4	1/4	0.55411(8)	92(3)
In1/Ni3	4*c*	34(1)/66(1)	3/4	1/4	0.90797(6)	97(5)
In2	8*g*	100	1/4	0.41397(7)	0.85631(3)	83(1)
$Y_{13.84(2)}Ni_{3.19(2)}In_{2.97(2)}$						
Y1/In3	4*c*	84(2)/16(2)	3/4	1/4	0.14545(6)	161(4)
Y2	4*d*	100	1/4	1/4	0.21433(6)	130(3)
Y3	8*g*	100	1/4	0.54522(11)	0.30578(4)	151(2)
Y4	8*g*	100	1/4	0.56406(11)	0.98318(4)	153(2)
Y5	8*f*	100	0.56421(7)	$-x$	1/4	142(2)
Y6	8*g*	100	1/4	0.43816(10)	0.46644(4)	132(2)
Y7	16*h*	100	0.43463(7)	0.43463(7)	0.10513(3)	128(1)
Ni1	8*g*	100	1/4	0.53552(15)	0.18927(6)	158(3)
Ni2	4*d*	100	1/4	1/4	0.55277(8)	148(4)
In1/Ni3	4*c*	81(2)/19(2)	3/4	1/4	0.90694(5)	130(4)
In2	8*g*	100	1/4	0.41171(7)	0.85472(3)	131(2)
$Gd_{14}Ni_{3.29(2)}In_{2.71(2)}$						
Gd1	4*c*	100	3/4	1/4	0.14539(3)	157(1)
Gd2	4*d*	100	1/4	1/4	0.21426(3)	147(1)
Gd3	8*g*	100	1/4	0.54690(5)	0.30622(2)	190(1)
Gd4	8*g*	100	1/4	0.56417(5)	0.98397(2)	175(1)
Gd5	8*f*	100	0.56342(3)	$-x$	1/4	154(1)
Gd6	8*g*	100	1/4	0.43853(5)	0.46642(2)	150(1)
Gd7	16*h*	100	0.43587(3)	0.43654(3)	0.10455(2)	144(1)
Ni1	8*g*	100	1/4	0.53580(14)	0.18875(6)	197(3)
Ni2	4*d*	100	1/4	1/4	0.55330(8)	181(4)
In1/Ni3	4*c*	71(2)/29(2)	3/4	1/4	0.90671(5)	159(4)
In2	8*g*	100	1/4	0.40747(7)	0.85491(3)	141(1)
$Tb_{13.82(2)}Ni_{3.36(2)}In_{2.82(2)}$						
Tb1/In3	4*c*	82(2)/18(2)	3/4	1/4	0.14486(5)	132(4)
Tb2	4*d*	100	1/4	1/4	0.21485(4)	117(2)
Tb3	8*g*	100	1/4	0.54710(7)	0.30690(3)	163(2)
Tb4	8*g*	100	1/4	0.56515(6)	0.98433(3)	155(2)
Tb5	8*f*	100	0.56557(5)	$-x$	1/4	131(2)
Tb6	8*g*	100	1/4	0.43913(6)	0.46603(3)	120(2)
Tb7	16*h*	100	0.43725(4)	0.43452(5)	0.10483(2)	117(1)
Ni1	8*g*	100	1/4	0.53510(19)	0.18888(9)	160(4)
Ni2	4*d*	100	1/4	1/4	0.55296(12)	146(5)
In1/Ni3	4*c*	64(2)/36(2)	3/4	1/4	0.90699(7)	138(6)
In2	8*g*	100	1/4	0.40935(9)	0.85489(4)	108(2)
$Dy_{13.60(2)}Ni_{3.34(2)}In_{3.06(2)}$						
Dy1/In3	4*c*	60(2)/40(2)	3/4	1/4	0.14438(5)	156(4)
Dy2	4*d*	100	1/4	1/4	0.21527(4)	134(2)
Dy3	8*g*	100	1/4	0.54696(7)	0.30660(3)	177(2)
Dy4	8*g*	100	1/4	0.56515(6)	0.98379(3)	180(2)
Dy5	8*f*	100	0.56626(5)	$-x$	1/4	157(2)
Dy6	8*g*	100	1/4	0.43855(6)	0.46553(3)	139(1)
Dy7	16*h*	100	0.43772(5)	0.43438(5)	0.10486(2)	141(1)
Ni1	8*g*	100	1/4	0.53448(19)	0.18877(9)	175(4)
Ni2	4*d*	100	1/4	1/4	0.55300(12)	162(5)
In1/Ni3	4*c*	66(2)/34(2)	3/4	1/4	0.90724(7)	153(6)
In2	8*g*	100	1/4	0.41022(9)	0.85459(4)	132(2)

Table 5 (*continued*)

Atom	Wyckoff site	Occupancy/%	x	y	z	U_{eq}
$Ho_{13.35(2)}Ni_{3.17(2)}In_{3.48(2)}$						
Ho1/In3	4*c*	35(4)/65(4)	3/4	1/4	0.14431(14)	229(14)
Ho2	4*d*	100	1/4	1/4	0.21554(11)	180(6)
Ho3	8*g*	100	1/4	0.5442(2)	0.30557(7)	201(4)
Ho4	8*g*	100	1/4	0.5649(2)	0.98213(7)	211(4)
Ho5	8*f*	100	0.56877(14)	$-x$	1/4	197(4)
Ho6	8*g*	100	1/4	0.4374(2)	0.46547(7)	187(4)
Ho7	16*h*	100	0.43823(16)	0.43346(16)	0.10520(4)	187(3)
Ni1	8*g*	100	1/4	0.5348(7)	0.1883(2)	210(12)
Ni2	4*d*	100	1/4	1/4	0.5530(3)	215(17)
In1/Ni3	4*c*	83(5)/17(5)	3/4	1/4	0.90727(17)	204(16)
In2	8*g*	100	1/4	0.4121(3)	0.85438(11)	178(6)
$Er_{13.53(2)}Ni_{3.14(2)}In_{3.33(2)}$						
Er1/In3	4*c*	53(2)/47(2)	3/4	1/4	0.14493(4)	136(3)
Er2	4*d*	100	1/4	1/4	0.21438(4)	115(1)
Er3	8*g*	100	1/4	0.54392(6)	0.30532(3)	133(1)
Er4	8*g*	100	1/4	0.56415(6)	0.98272(3)	140(1)
Er5	8*f*	100	0.56749(4)	$-x$	1/4	129(1)
Er6	8*g*	100	1/4	0.43848(5)	0.46633(3)	120(1)
Er7	16*h*	100	0.43784(4)	0.43346(4)	0.10513(2)	117(1)
Ni1	8*g*	100	1/4	0.53592(17)	0.18829(8)	141(3)
Ni2	4*d*	100	1/4	1/4	0.55347(10)	128(4)
In1/Ni3	4*c*	86(2)/14(2)	3/4	1/4	0.90689(6)	117(5)
In2	8*g*	100	1/4	0.41149(8)	0.85452(4)	114(2)
$Tm_{13.47(3)}Ni_{3.28(3)}In_{3.25(3)}$						
Tm1/In3	4*c*	47(2)/53(2)	3/4	1/4	0.14435(8)	102(6)
Tm2	4*d*	100	1/4	1/4	0.21484(6)	64(3)
Tm3	8*g*	100	1/4	0.54542(12)	0.30628(4)	101(2)
Tm4	8*g*	100	1/4	0.56399(11)	0.98344(5)	106(2)
Tm5	8*f*	100	0.56663(8)	$-x$	1/4	83(2)
Tm6	8*g*	100	1/4	0.43887(11)	0.46587(4)	76(2)
Tm7	16*h*	100	0.43789(8)	0.43382(8)	0.10505(3)	72(2)
Ni1	8*g*	100	1/4	0.53511(34)	0.18864(13)	96(6)
Ni2	4*d*	100	1/4	1/4	0.55352(18)	80(8)
In1/Ni3	4*c*	72(3)/28(3)	3/4	1/4	0.90736(11)	63(9)
In2	8*g*	100	1/4	0.41183(17)	0.85466(7)	66(3)
$Tm_{13.80(2)}Ni_{3.49(2)}In_{2.71(2)}$						
Tm1/In3	4*c*	80(2)/20(2)	3/4	1/4	0.14504(4)	118(3)
Tm2	4*d*	100	1/4	1/4	0.21459(3)	107(2)
Tm3	8*g*	100	1/4	0.54847(7)	0.30851(3)	155(1)
Tm4	8*g*	100	1/4	0.56544(6)	0.98597(3)	134(1)
Tm5	8*f*	100	0.56498(4)	$-x$	1/4	110(1)
Tm6	8*g*	100	1/4	0.44165(6)	0.46647(2)	115(1)
Tm7	16*h*	100	0.43676(4)	0.43346(4)	0.10501(2)	101(1)
Ni1	8*g*	100	1/4	0.53371(19)	0.19027(8)	139(3)
Ni2	4*d*	100	1/4	1/4	0.55278(10)	114(4)
In1/Ni3	4*c*	51(2)/49(2)	3/4	1/4	0.90781(7)	125(7)
In2	8*g*	100	1/4	0.41170(9)	0.85561(4)	99(2)
$Lu_{13.94(2)}Ni_{3.07(2)}In_{2.99(4)}$						
Lu1/In3	4*c*	94(2)/6(2)	3/4	1/4	0.14532(4)	96(3)
Lu2	4*d*	100	1/4	1/4	0.21202(4)	87(2)
Lu3	8*g*	100	1/4	0.54383(7)	0.30495(3)	109(1)
Lu4	8*g*	100	1/4	0.55982(6)	0.96793(3)	95(1)
Lu5	8*f*	100	0.56350(5)	$-x$	1/4	102(1)
Lu6	8*g*	100	1/4	0.43793(6)	0.48377(3)	99(1)
Lu7	16*h*	100	0.43621(4)	0.43462(5)	0.10497(2)	88(1)
Ni1	8*g*	100	1/4	0.5377(2)	0.18903(9)	127(4)
Ni2	4*d*	100	1/4	1/4	0.55377(11)	106(5)
In1/Ni3	4*c*	93(2)/7(2)	3/4	1/4	0.90651(6)	91(5)
In2	8*g*	100	1/4	0.41077(11)	0.85501(4)	94(2)

Table 6
Interatomic distances (pm), in $Gd_{14}Ni_{3.29(2)}In_{2.71(2)}$

Gd1	2	In2	330.6	Gd5	2	In2	338.9	Ni1	1	Gd3	274.0
	2	Gd4	350.8		2	Gd3	346.5		1	Gd2	282.2
	4	Gd5	352.6		2	Ni1	348.0		2	Gd7	282.6
	4	Gd7	365.3		2	Gd1	352.6		2	Gd3	285.2
Gd2	2	Ni1	282.2		2	Gd5	360.2		1	In1/Ni3	303.7
	2	Gd3	357.9		2	Gd7	360.7		2	Gd5	348.0
	4	Gd7	360.6		2	Gd2	361.8	Ni2	2	Gd6	272.2
	2	In2	361.3	Gd6	1	Ni2	272.2		4	Gd7	280.9
	4	Gd5	361.8		1	In1/Ni3	331.3		2	Gd4	343.6
	1	Ni2	375.1		2	In2	351.8		1	Gd2	375.1
Gd3	1	Ni1	274.0		2	Gd4	356.0	In1/Ni3	2	Ni1	303.7
	2	Ni1	285.2		1	Gd6	364.0		2	Gd3	305.4
	1	In1/Ni3	305.4		2	Gd7	365.5		2	Gd4	311.6
	2	In2	343.7		2	Gd4	368.7		2	Gd6	331.3
	2	Gd5	346.5		2	Gd7	368.9		4	Gd7	352.8
	1	Gd2	357.9		1	Gd3	387.7	In2	1	In2	304.0
	2	Gd7	367.5	Gd7	1	Ni2	280.9		1	Gd1	330.6
	2	Gd3	381.5		1	Ni1	282.6		1	Gd4	336.7
	1	Gd6	387.7		1	In2	351.5		2	Gd5	338.9
	1	Gd3	392.1		1	In1/Ni3	352.8		2	Gd3	343.7
Gd4	1	In1/Ni3	311.6		1	Gd4	355.4		2	Gd7	351.5
	1	In2	336.7		1	Gd7	358.9		2	Gd6	351.8
	1	Ni2	343.6		1	Gd7	360.1		1	Gd2	361.3
	1	Gd1	350.8		1	Gd2	360.6				
	2	Gd7	355.4		1	Gd5	360.6				
	2	Gd6	356.0		1	Gd1	365.3				
	1	Gd4	358.8		1	Gd6	365.5				
	2	Gd7	366.7		1	Gd4	366.7				
	2	Gd6	368.7		1	Gd3	367.5				
					1	Gd6	368.9				

Standard deviations are all equal or less than 0.2 pm. All distances within the first coordinate spheres are listed.

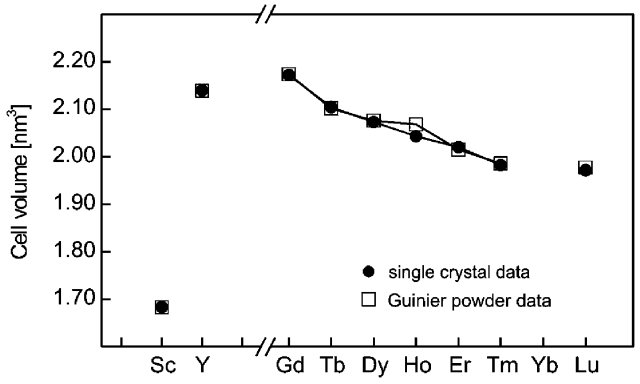

Fig. 1. Plot of the cell volumes of the tetragonal $RE_{14}Ni_3In_3$ indides.

the average Gd–Gd distance of 360 pm in *hcp* gadolinium [24]. We can thus assume a considerable degree of Gd–Gd bonding in this intermetallic compound.

The polyhedra of Gd1, Gd2, Gd4, Gd5, Gd6, and Gd7 derive from slightly distorted pentagonal prisms formed by the ten nearest gadolinium neighbors. These prisms are capped on the pentagonal and rectangular sides by the additional nickel and indium neighbors, resulting in the higher coordination numbers. The coordination polyhedron of Gd3 is the most irregular one. Only parts of this coordination polyhedron derive from an icosahedron.

Both nickel sites have a tri-capped trigonal prismatic coordination. The trigonal prisms are formed by gadolinium atoms for both Ni1 and Ni2. While three gadolinium atoms are capping the prisms of Ni2, two Gd + 1 Ni/In atoms take these positions for Ni1. This tri-capped trigonal prismatic coordination is typically observed for the transition metal atoms in rare earth–transition metal–indides [1]. Especially in the equiatomic *RE*NiIn indides [1,26] with hexagonal ZrNiAl-type structure, the Ni2 atoms have a trigonal prismatic rare earth coordination. The Ni–Gd distances from the central nickel atoms to the gadolinium atoms building the trigonal prisms range from 272 to 285 pm, close to the sum of the covalent radii of 276 pm (Gd + Ni) [25]. These interactions can be considered as strongly bonding.

The 4*c* site shows a mixed occupancy by 71% In and 29% Ni (Table 5). Such mixed Ni/In occupancies have recently been observed for a variety of compounds like the series $TmNi_{1-x-y}In_{1+x}$ [18], $Sc_3Ni_{2.10(5)}In_{3.60(5)}$, or $Sc_3Ni_{2.14(2)}In_{3.76(2)}$ [16]. The mixed occupied site has coordination number 12 by ten gadolinium and two

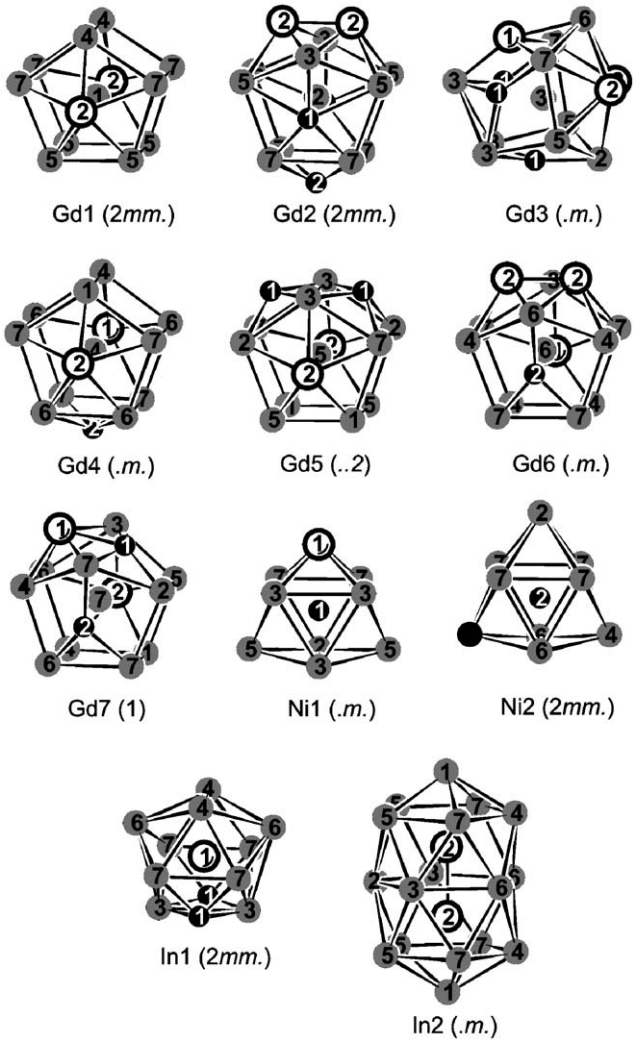

Fig. 2. Coordination polyhedra in the $Gd_{14}Ni_{3.29(1)}In_{2.71(1)}$ structure. Gadolinium, nickel, and indium atoms are drawn as gray, black filled, and open circles, respectively. Atoms marked with a crescent indicate Ni/In mixing. The site symmetries are indicated.

nickel atoms. The In1/Ni3–Ni1 distance of 304 pm is significantly larger than the sum of the covalent radii for Ni + In of 265 pm [25]. In view of the high indium occupancy on this site, one has to consider the nearest gadolinium neighbors (305 and 312 pm), which are close to the sum of the covalent radii of 311 pm (Gd + In) [25].

The most remarkable feature of the $Gd_{14}Ni_{3.29}In_{2.71}$ structure is the coordination polyhedron of the In2 atoms (Fig. 2). Each In2 atom has 11 gadolinium and one In2 neighbors in slightly distorted icosahedral coordination. Always two of these icosahedra interpenetrate, forming the building unit shown in Fig. 2. The centeral indium atom of one icosahedron acts as the capping atom of the second one. This way we obtain a dumb-bell of In2 atoms at an In2–In2 distance of 304 pm, much shorter than in tetragonal body-centered elemental indium (4×325 and 8×338 pm) [24]. This segregation is surprising. In view of the enormous gadolinium content (the $RE_{14}Ni_3In_3$ intermetallics are the so far most rare earth metal-rich $RE_xT_yIn_z$ compounds [1]) one would expect a separation of the indium atoms.

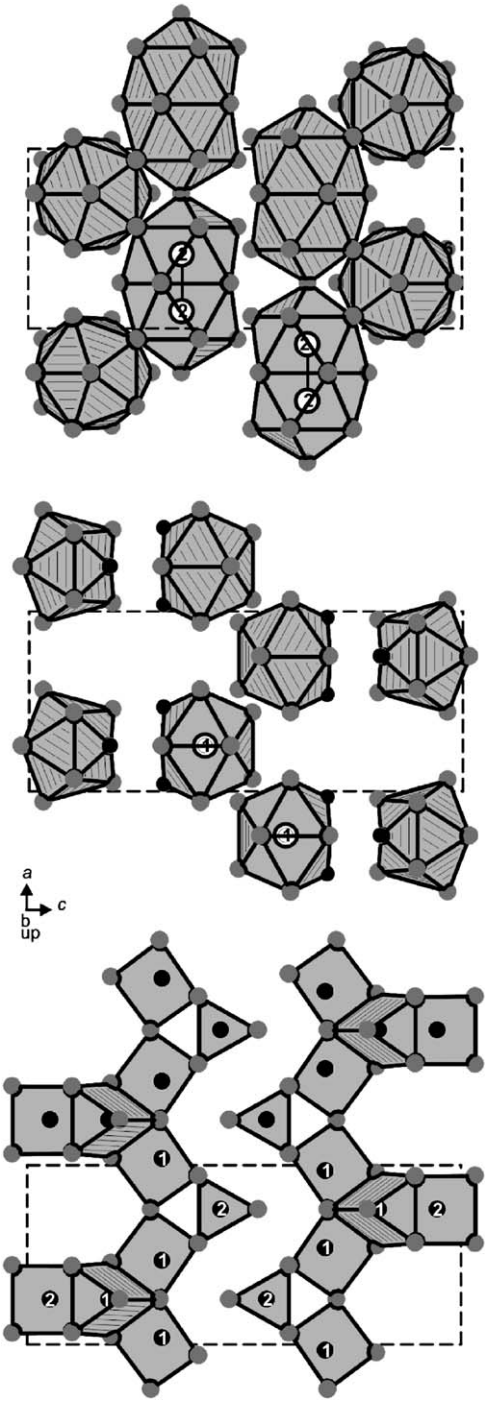

Fig. 3. View of the $Gd_{14}Ni_{3.29(2)}In_{2.71(2)}$ structure along the *b*-axis. The characteristic coordination polyhedra around the In2 (upper part), In1/In3 (middle), Ni1, and Ni2 (lower part) atoms are drawn. Atoms that do not belong to these polyhedral units are omitted for clarity. For details see text.

Finally we discuss the complete structure of $Gd_{14}Ni_{3.29}In_{2.71}$ via the packing of the different polyhedra. In Fig. 3 we present three different structural motifs. In the upper part of that drawing the condensed icosahedra around the indium atoms are emphasized. The Gd1 atoms capping the double unit have a pentagonal prismatic coordination. Thus we obtain columns of pentagonal antiprisms ($2\times$) that alternate with pentagonal prisms. Due to the 4_2 screw axis, these one-dimensional columns extend in the *a* or the *b* direction.

The second characteristic building unit is shown in the middle of Fig. 3. The mixed occupied In1/Ni3 position has coordination number 12. In the lower part of that drawing the trigonal gadolinium prisms around the two crystallographically independent nickel sites are drawn. The latter are condensed via common corners and edges. These three building units comprise all atoms of the $Gd_{14}Ni_{3.29}In_{2.71}$ structure. Since that intergrowth is complicated, we prefer the separate drawings for reasons of clarity.

Acknowledgments

We are grateful to Dr. R.-D. Hoffmann for help with the intensity data collections and to H.-J. Göcke for the work at the scanning electron microscope. This work was supported by the Deutsche Forschungsgemeinschaft. M.L. is indebted to the NRW Graduate School of Chemistry for a Ph.D. stipend and Y.G. is indebted to the DAAD for a research stipend.

References

[1] Ya.M. Kalychak, V.I. Zaremba, R. Pöttgen, M. Lukachuk, R.-D. Hoffmann, Rare earth-transition metal-indides, in: K.A. Gschneidner Jr., V.K. Pecharsky, J.-C. Bünzli (Eds.), Handbook on the Physics and Chemistry of Rare Earths, vol. 34, Elsevier, Amsterdam, 2005, pp. 1–133 (Chapter 218).
[2] R.-D. Hoffmann, R. Pöttgen, Chem. Eur. J. 6 (2000) 600.
[3] R.-D. Hoffmann, R. Pöttgen, V.I. Zaremba, Ya.M. Kalychak, Z. Naturforsch. 55b (2000) 834.
[4] Ya.M. Kalychak, V.I. Zaremba, Ya.V. Galadzhun, Kh.Y. Milianchuk, R.-D. Hoffmann, R. Pöttgen, Chem. Eur. J. 7 (2001) 5343.
[5] Ya.M. Kalychak, V.I. Zaremba, A. Stępień-Damm, Ya.V. Galadzhun, L.G. Akselrud, Kristallografia 43 (1998) 17 (in Russian).
[6] Ya.M. Kalychak, J. Alloys Compd. 262–263 (1997) 341.
[7] Ya.M. Kalychak, J. Alloys Compd. 291 (1999) 80.
[8] Ya.M. Kalychak, V.I. Zaremba, P.Yu. Zavalii, Z. Kristallogr. 208 (1993) 380.
[9] V.I. Zaremba, Ya.M. Kalychak, P.Yu. Zavalii, Sov. Phys. Crystallogr. 37 (1992) 178.
[10] M. Lukachuk, Ya.M. Kalychak, M. Dzevenko, R. Pöttgen, J. Solid State Chem. 178 (2005) 1247.
[11] Ya.V. Galadzhun, V.I. Zaremba, Ya.M. Kalychak, V.M. Davydov, A.P. Pikul, A. Stępień-Damm, D. Kaczorowski, J. Solid State Chem. 177 (2004) 17.
[12] F. Canepa, M. Napoletano, M.L. Fornasini, F. Merlo, J. Alloys Compd. 345 (2002) 42.
[13] V.I. Zaremba, Ya.M. Kalychak, V.P. Dubenskiy, R.-D. Hoffmann, R. Pöttgen, J. Solid State Chem. 152 (2000) 560.
[14] V.I. Zaremba, Ya.M. Kalychak, Yu.B. Tyvanchuk, R.-D. Hoffmann, M.H. Möller, R. Pöttgen, Z. Naturforsch. 57b (2002) 791.
[15] V. Hlukhyy, V.I. Zaremba, Ya.M. Kalychak, R. Pöttgen, J. Solid State Chem. 177 (2004) 1359.
[16] M. Lukachuk, V.I. Zaremba, R.-D. Hoffmann, R. Pöttgen, Z. Naturforsch. 59b (2004) 182.
[17] V.I. Zaremba, V. Hlukhyy, R. Pöttgen, Z. Anorg. Allg. Chem. 631 (2005) 327.
[18] M. Lukachuk, Ya.M. Kalychak, R. Pöttgen, Z. Naturforsch. 59b (2004) 893.
[19] V.I. Zaremba, I.R. Muts, U.Ch. Rodewald, V. Hlukhyy, R. Pöttgen, Z. Anorg. Allg. Chem. 630 (2004) 1903.
[20] M. Lukachuk, Ya.M. Kalychak, R. Pöttgen, R.-D. Hoffmann, Z. Kristallogr. Suppl. 20 (2003) 142.
[21] R. Pöttgen, Th. Gulden, A. Simon, GIT-Laborfachzeitschrift 43 (1999) 133.
[22] K. Yvon, W. Jeitschko, E. Parthé, J. Appl. Crystallogr. 10 (1977) 73.
[23] G.M. Sheldrick, SHELXL-97, Program for Crystal Structure Refinement, University of Göttingen, Germany, 1997.
[24] J. Donohue, The Structures of the Elements, Wiley, New York, 1974.
[25] J. Emsley, The Elements, Oxford University Press, Oxford, 1999.
[26] R. Ferro, R. Marazza, G. Rambaldi, Z. Metallkd. 65 (1974) 37.